Vibrational spectra of a-Si:H, a-Si:F, and a-Ge:F: Bethe-lattice calculations

E. Martínez* and Manuel Cardona

Max-Planck-Institut für Festkörperforschung, Heisenbergstrasse 1,
D-7000 Stuttgart 80, Federal Republic of Germany
(Received 4 March 1983)

The local densities of vibrational states around Si-H and Si-F bands in a-Si are obtained by means of a cluster-Bethe-lattice calculation. Nearest-neighbor bond-stretching and -bending constants are included. The calculations reproduce the peaks observed in the ir spectra of both a-Si:H and a-Si:F near the upper edge of the TA band (~ 210 cm^{-1}). As a result of the calculation, these peaks, however, are seen to have a different origin in the case of a-Si:H and a-Si:F. In the former, the peak is a resonance vibrating longitudinally to the bond with the H atom rigidly attached to the Si neighbor. For the a-Si:F case the resonance has transverse character and corresponds to a mixture of wagging modes of the Si—F bond and TA modes of the a-Si matrix. Published ir spectra of a-Si:H must be correspondingly interpreted. A calculation of the ir spectrum of a-Si:F, in which the absorption strength is not an adjustable parameter, is presented and compared with experiment. The calculations for a-Si:F are extended to a-Ge:F.

I. INTRODUCTION

The ir and Raman spectra of a-Ge and a-Si have been very useful for the characterization of these materials and their hydrogenated and fluorinated versions [a-Si:(H,F); a-Ge:(H,F)].[1,2] Local modes of the Si—H, Ge—H, Si—F, and Ge—F bonds, with the self-explanatory labels of stretching, bending, and wagging, are usually found next to a broad, continuous spectrum due to the Si (Ge) matrix. The continuous spectrum shows four peaks or shoulders which correspond to the TA, LA, LO, and TO branches of the crystalline materials. This spectrum, strictly forbidden in the pure crystals for these nonpolar materials, becomes allowed in the amorphous counterparts due to disorder. The presence of the strongly electronegative fluorine impurities have been seen to enhance this ir absorption.[3]

Recently, a sharp resonance or quasilocal mode has been observed near the top of the TA bands of a-Si:H, a-Ge:H,[4,5] and a-Si:F.[3] They were recognized in Ref. 4 as being related to the singularity of the density of states which exists near the W point of the Brillouin zone in c-Si. The details of this correlation, which—as will be seen below—seems to be basically correct, are, however, somewhat obscure. In Ref. 4 the correlation was obtained by means of a mass-defect local-mode calculation using, as the mass defect, four hydrogen atoms. While this procedure may be meaningful for hydrogen, it certainly does not apply to fluorine because of its heavier mass.

Another attempt to explain these quasilocal modes for Si-H was made in Ref. 6 with a Bethe-lattice technique. It was concluded in this paper that the local mode appears if several hydrogen atoms are clustered together on a plane to form an incipient [111] surface. However, some difficulties arose in the evaluation of the oscillator strength for such a model.

In this paper we calculate the local densities of vibrational states for the Si and H (F) of a Si—H (Si—F) bond with the silicon tied to three other Si atoms connected to a Bethe lattice (cluster-Bethe-lattice method[7,8]). Calculations are also performed for a-Ge:F. In the Si case, a

peak, corresponding to the quasilocal mode discussed above, can be obtained in the density of states (DOS) for the longitudinal component of the —Si—H vibration (Si and H move almost together) for reasonable parameters of the force constants. In the a-Si:F case the corresponding vibration is actually transverse polarized and the Si and H atoms do not move rigidly. The nature of the vibration is thus completely different from the one above although the peak in the DOS is similar. Because of this difference we are able to perform a quantitative calculation of the absorption spectrum of a-Si:F using for the effective changes molecular data for SiF$_4$. The calculated spectra agree rather well with experimental data. Similar calculations are performed for a-Ge:F. No experimental data are available in this case for comparison.

II. CALCULATIONS

In the following sections we calculate the local phonon density of states for the defects in a-Si sketched in Fig. 1, in which atom X can be either an F or an H atom, or just nothing for the case of a vacancy. Since we deal mainly with in-band resonance states, it is necessary that the three Si atoms connected to the amorphous Si network can vi-
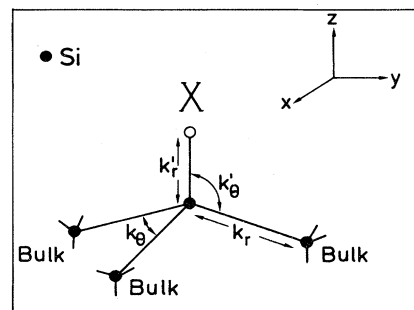

FIG. 1. Diagram of the force constants of the simple model of Table I used for the calculation of vibrational frequencies in bulk Si, Si surfaces, a-Si:H, and a-Si:F.

brate in a bulk environment to reproduce suitably the interaction with the continuous spectrum of the bulk. This is achieved using the cluster-Bethe-lattice method,[7,8] in which every dangling bond of the Si atoms in the boundary of the cluster of interest is saturated with an infinite Si Bethe lattice. We use a valence-force-field model Hamiltonian for which the potential energy of deformation of the system is given by

$$U = \frac{1}{2} \sum_i \left[\sum_j K_r(i,j)(\delta r_{ij})^2 \right.$$
$$\left. + \sum_{j,k} R_{ij} R_{ik} K_\theta(j,i,k)(\delta\theta_{jik})^2 \right] , \quad (1)$$

where δr_{ij} and $\delta\theta_{jik}$ are the variation of the distance between atoms i and j and the angle formed by atoms j, i, and k, respectively. R_{ij} is the equilibrium bond length. The index i runs over all atoms of the system and j and k run over the first nearest neighbors of atom i. This Hamiltonian includes two types of interactions: the stretching-stretching force constants $K_r(i,j)$ for the $i-j$ bonds and the bond bending-bending force constants $K_\theta(i,j,K)$ for the $i-j-k$ bond angle. In our calculations we consider only four different force constants for each system which we will designate as K_r and K_θ for the Si bulk and K_r' and K_θ' for the Si—X bond and X—Si—Si bond angle, respectively. These interactions are schematically represented in Fig. 1. The Si Bethe lattice has been solved using the transfer-matrix method.[8] Since the Hamiltonian described above includes second-neighbor interactions, we have used a generalization of this method similar to one recently developed[9] for an electronic tight-binding Hamiltonian. Details of this method and its application to this particular cluster calculations are described in the Appendix. The bulk vibrational density of states obtained with this Bethe lattice is shown in Fig. 2, using the parameters K_r and K_θ of Table I. These parameters have been chosen to fit the center of the TO band (~ 480 cm^{-1}) and the upper edge of the TA band (~ 210 cm^{-1}). This density of states reproduces qualitatively the Raman spectrum of a-Si except for two features. First, it does not reproduce the two humps observed in the longitudinal acoustical and optical bands due to the absence of closed rings of bonds in the Bethe lattice.[8] Therefore, the behavior of these features with the incorporation of H or F cannot be properly described in this approximation. Nevertheless, an analysis of the correlation functions reveals that the transition from an acousticlike into an opticlike longitudinal band at ~ 355 cm^{-1} is present in this density of states. Second, the Bethe lattice does not satisfy the acoustic limit, having an unphysical lower edge of the TA band at ~ 70 cm^{-1}. Therefore, those defect modes which may appear near the low-frequency edge of the spectrum have to be regarded with caution.

This effective medium is connected to the cluster of Fig. 1 and the 3×3 $\overset{\leftrightarrow}{G}_{ij}$ matrices are calculated, where $\overset{\leftrightarrow}{G}_{ij}$ is the set of matrix elements of the Green's function between atoms i and j as described in the Appendix. The local density of states (LDOS) in atom i is given by

$$N_i(\omega) = -\frac{2M\omega}{\pi} \lim_{\eta \to 0} \mathrm{Im}[\mathrm{Tr}\overset{\leftrightarrow}{G}_{ii}(\omega^2 + i\eta)] , \quad (2)$$
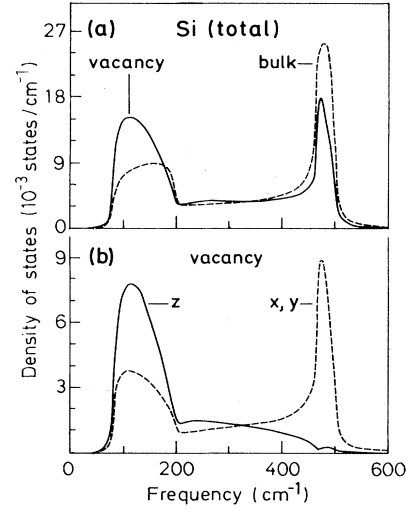

FIG. 2. Densities of vibrational states for a Si atom near a vacancy as obtained by the Bethe-lattice technique. These results are compared with the bulk densities of states. The z coordinate points towards the vacancy. The results for the vacancy qualitatively agree with the calculation by the recursion method performed by K. Suzuki, D. Schmeltzer, and A. A. Maradudin [J. Phys. (Paris) Colloq. C6, 42 (1981)].

and the correlation function between the displacements of atoms i and j is

$$\langle \vec{U}_i \cdot \vec{U}_j \rangle = -\frac{\hbar\omega}{\pi} \lim_{\eta \to 0} \mathrm{Im}\overset{\leftrightarrow}{G}_{ij}(\omega^2 + i\eta) . \quad (3)$$

III. RESULTS

A. Vacancy

For the purpose of comparison we show in Fig. 2 the local density of vibrational states for a Si atom near to a vacancy, i.e., in a defect such as that of Fig. 1 when atom X is removed. The main change we can observe with respect to the bulk density of states is a transfer of about one third of the states of the TO band to the TA band. In Fig. 2(b) we show the local density of states (LDOS) in the Si atom of the vacancy projected on the z and x, y directions, using the coordinate axes of Fig. 1. Because of symmetry, these three projections are identical for a bulk Si atom. As can be easily understood the vibrations in the xy plane are only slightly perturbed, however, the bulk states corresponding to vibrations of the Si atom against its neighbor in the Z direction are shifted to lower frequencies near the vacancy. Notice that we are dealing with an ideal nonrelaxed vacan-

TABLE I. Force constants used in the present paper (with the exception of Fig. 8, see text) in 10^5 dyn cm^{-1}.

	K_r	K_θ	K_r'	K_θ'
a-Si:H	1.3	0.042	2.28	0.092
a-Si:F	1.3	0.042	4.4	0.12
a-Ge:H	1.16	0.036	2.09	0.077
a-Ge:F	1.16	0.036	4.04	0.1

cy and that we have not taken into account the possible interaction between the dangling bond and the back bonds. The latter would only be physically meaningful in a bond-charge description.[10]

B. Si—H

In order to calculate the vibrational density of states when an H atom is attached to a Si dangling bond in a-Si, we include two new force constants K_r' and K_θ' as described in the preceding section. In the case of the Si—H bond these two new parameters are fitted to the wagging (~ 630 cm^{-1}) and stretching (~ 2000 cm^{-1}) frequencies observed in[1,2,11] ir and Raman[5] spectra. The values of these force constants are given in Table I. In Fig. 3 we show the local density of vibrational states for the H atom and for the Si atom attached to it. The correlation function G_{Si-H} is positive in all the frequency range displayed in the figure and in the x, y, and z directions. Thus, these states correspond to vibrations in which the Si and H atoms move in the same direction. A comparison of Figs. 3 and 2 reveals that the H atom induces two main features in the vibrational spectrum of a Si atom near a vacancy. (i) The states corresponding to vibrations in the Si—H bond direction are shifted to higher frequencies and have the tendency to accumulate near the upper edge of the TA band. This shift can be easily understood considering the resistance to deformation of the bond angles Si—Si—H, introduced by the new force constant K_θ'. The small mass of the H atom is not large enough to shift these states down and plays no role in the vibrations of the cluster. The z component of the vibration shows a weak peak close to 200 cm^{-1}. This peak depends very critically on the force constants chosen and can be enhanced if the constants of the Si—Si backbonds are slightly increased (see discussion). We should point out that a first-neighbor interaction Hamiltonian is not able to reproduce this feature, a fact which led to the introduction of the model of Ref. 6. (ii) The vibrations perpendicular to the Si—H bond are only perturbed in the TO band centered at 480
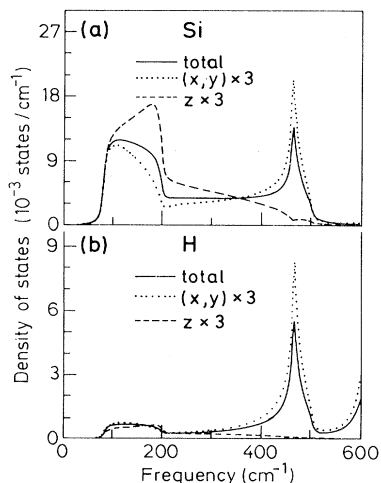

FIG. 3. Density of vibrational states for the Si and H atom of a-Si—H bond in a-Si as obtained with the Bethe-lattice method using the parameters of Table I.

cm^{-1} in the vacancy. We can observe a splitting of these states: Some of them shift to the wagging-mode frequency at 630 cm^{-1}, whereas the rest shift slightly to lower frequencies at ~ 460 cm^{-1}. Finally, we can also see in Fig. 3(b) that the relative weights of the TO and TA bands of the LDOS on the H atom are different from those for the Si atom, the TO band states being enhanced by the wagging mode in the H states. As we shall see later, this is relevant to interpret the neutron scattering experiments.

C. Si—F

Ir experiments[12,13] indicate that the stretching frequency for the Si—F bond in a-Si is at ~ 830 cm^{-1}. This value has been used to fit the K_r' force constant of Table I. However, the wagging-mode frequency, which would allow us to fit the force constant K_θ', cannot be easily extracted from the experiments. Extrapolations from molecular data show that, due to the large mass of the F atom, this mode is inside the bulk continuum spectrum of a-Si and so we can expect it to interact strongly with the vibrations of the Si atoms. Four peaks have been observed[3,12,13] below 520 cm^{-1}, associated with the presence of F in a-Si, at about 510, 380, 300, and 212 cm^{-1}. The peak at 380 cm^{-1} can be clearly assigned to the bending mode of the SiF$_n$ molecule due to its annealing behavior.[12] The peak at 212 cm^{-1} was associated with the same mechanism that gives rise to a peak at the same frequency in a-Si:H; the peak at 510 cm^{-1} was considered to be a perturbed TO Si vibration induced by the presence of F, whereas the wagging mode was ascribed to the peak at 300 cm^{-1}. These assignments had two main problems: First, none of the mechanisms proposed[4,6,14] to explain the "quasilocal" mode at 210 cm^{-1} in a-Si:H work satisfactorily in the case of a-Si:F and, second, it is difficult to understand why the ir activity[3] of the wagging mode of the rather ionic Si—F bond is smaller than that of the other resonance modes.

In order to clarify the position of the Si-F wagging mode and to study its interaction with the bulk continuum spectrum we have calculated the density of vibrational states in the cluster of Fig. 1 embedded in a bulk Si Bethe lattice, for different bond-bending force constants. In Fig. 4 we show the evolution of the total density of vibrational states in the five-atom cluster when K_θ' is decreased. For an extremely high value of K_θ' (0.4 dyn cm^{-1}) we can see the wagging mode as a localized peak at ~ 550 cm^{-1}, above the bulk spectrum. For smaller values of the K_θ' force constant two main features should be noticed: First, this localized peak interacts strongly with the TO band, shifting its center to higher frequencies and becoming a strong resonance mode at ~ 505 cm^{-1} for small enough values of the bond-bending force constant. Second, the interaction of the F atom with the bulk spectrum produces a broad resonance in the longitudinal Si band that moves towards lower frequencies with decreasing values of K_θ'. When the TO resonance mode is at about 505 cm^{-1}, that latter feature appears as a sharp resonance mode in the TA-band upper edge, near 200 cm^{-1}. As will be shown below these two resonances correspond to wagginglike vibration modes and can be considered as the result of the interaction of the Si-F wagging mode with the Si bulk. The value of K_θ' given in Table I has been chosen to fit simultaneously the 212- and 510-cm^{-1} experimental
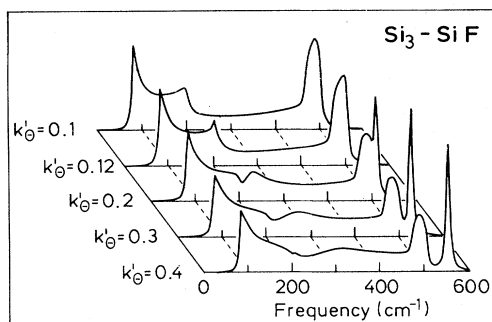
FIG. 4. Evolution of the total density of vibrational states in the five-atom cluster Si$_3$-SiF, embedded in a-Si, with the bond-bending force constant K'_θ (see Fig. 1).

peaks, and will be the value used in the following calculations. In order to analyze the characteristics of these resonance modes we show in Fig. 5 and Fig. 6 the local density of vibrational states in the Si and F atoms of the Si—F bond, respectively, as well as the projected density of states on the z and x,y directions of the coordinate system of Fig. 1. We also show in Fig. 7 the correlation function of the vibrations of the Si and F atoms. From these results we deduce the following main characteristics of the F-induced resonant modes in the Si spectrum. (i) The vibrations in the direction of the Si—F bond (z direction) are mainly in-phase vibrations, i.e., the Si and F atoms move together. The vibrations of the Si atom in this direction in a vacancy are not appreciably perturbed by the presence of the F atom (compare with Fig. 2). Although the new force constant K'_θ would push these states to higher energy, as in the case of the Si—H bond, this effect, however, is compensated by the larger mass of the F atom. (ii) The in-phase vibration modes in the x-y plane are in the region of the spurious TA-band lower edge of the Bethe lattice. Owing to this fact, the low-frequency states appear in our calculation as a sharp peak. We expect, however, that with a better description of the low-frequency region of
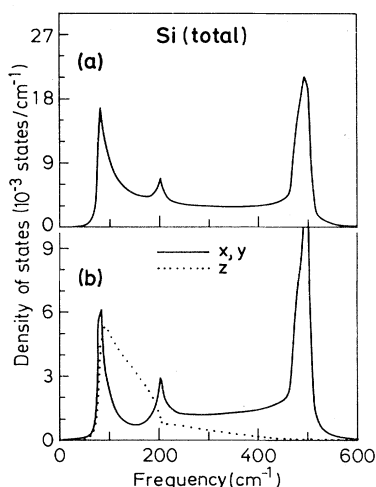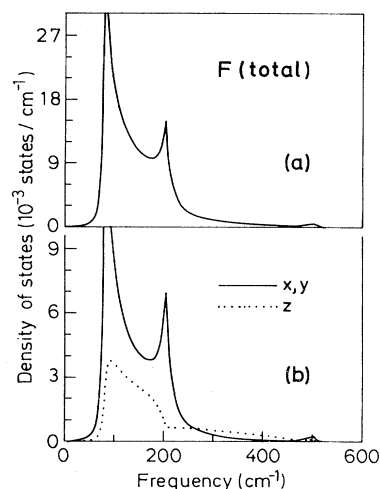

FIG. 6. Same as Fig. 5 but for the F atom.

the bulk continuum, those states should give rise to a broader resonance. (iii) The peaks at 208 and 505 cm^{-1} correspond both to vibrations in opposite phase in the direction perpendicular to the Si—F bond. The former is associated mainly with displacements of the F atom, whereas the latter corresponds to vibrations of the Si atom. (iv) All the vibrational states of the F atom are in the frequency region of the TA Si band, except for the stretching mode localized at 830 cm^{-1} (not displayed in the figures).

IV. DISCUSSION

The gross features of the perturbations in the bulk density of states induced by the presence of a vacancy, an F or an H atom, as described in the last section, are easy to understand if one considers the four vibrational modes of the molecule of Fig. 1 with an infinite mass for the "bulk" atoms. Two of them are doubly degenerate modes corresponding to vibrations in the xy plane whereas the other two correspond to vibrations in the z direction (see Table

FIG. 5. Partial (along x,y,z) and total densities of states for the vibration of Si in a-Si—F bond embedded in a-Si.
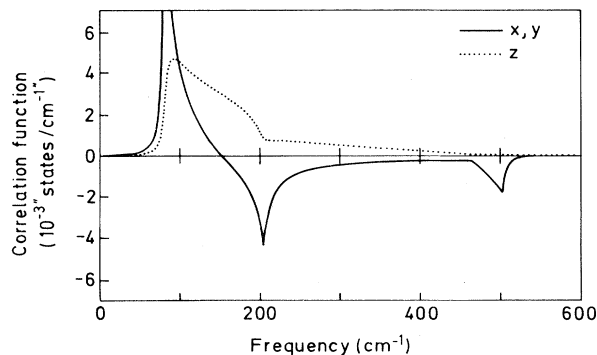

FIG. 7. Correlation function for the motion of Si and F in the same situation as Fig. 5. The vertical scale has been chosen to have the same normalization as those of Figs. 5 and 6, under the assumption that Figs. 5 and 6 represent G_{Si-Si} and G_{F-F}, respectively, while Fig. 7 represents G_{F-Si}.

II). The frequencies are given by the solutions of

$$(\omega_1^{xy}\omega_2^{xy})^2 = \frac{2}{M_{Si}M_X}\frac{1}{\beta}K'_\theta(K_r+2K_\theta) , \qquad (2a)$$

$$(\omega_1^{xy})^2+(\omega_2^{xy})^2 = \frac{4}{3M_{Si}}(K_r+2K_\theta)$$
$$+\left[\frac{3}{2}\frac{1}{\mu\beta}+\frac{1}{M_{Si}}\left[1+\frac{\beta}{6}\right]\right]K'_\theta , \qquad (2b)$$

$$(\omega_1^z\omega_2^z)^2 = \frac{1}{3M_{Si}M_X}K'_r(K_r+8K_\theta+8\beta K'_\theta) , \qquad (2c)$$

$$(\omega_1^z)^2(\omega_2^z)^2 = \frac{1}{3M_{Si}}(K_r+8K_\theta+8\beta K'_\theta)+\frac{1}{\mu}K'_r , \qquad (2d)$$

where μ and β are the reduced mass and the ratio of bond lengths, i.e.,

$$\mu^{-1}=M_{Si}^{-1}+M_X^{-1}$$
$$\beta=\frac{R_{Si-X}}{R_{Si-Si}} \qquad (3)$$

In this simplified scheme, the bulk can be approximately simulated by setting $M_X=\infty$, $\beta=1$, and $K'_{r,\theta}=K_{r,\theta}$ and the vacancy by setting $K'_{r,\theta}=0$. For the bulk we thus find a triply degenerate mode at

$$(\omega_2^{bulk})^2 = \frac{4}{3M_{Si}}(K_r+4K_\theta) , \qquad (4)$$

and a triply degenerate zero-frequency mode, which can be easily related to the optic and acoustic modes of Fig. 2, respectively. For the vacancy the zero-frequency modes are not perturbed, whereas the optic modes of (4) split into a double and a single degenerate mode given by

$$(\omega_2^{xy})^2 = \frac{4}{3M_{Si}}(K_r+2K_\theta) \qquad (5a)$$

$$(\omega_2^z)^2 = \frac{1}{3M_{Si}}(K_r+8K_\theta) . \qquad (5b)$$

As can be seen in Table II, the degenerate mode, corresponding to vibrations in the xy plane, is only slightly perturbed with respect to the bulk. However, the vibration in the z direction shifts to ~ 182 cm^{-1}, i.e., it overlaps with the TA band. This explains the transfer of one-third of the states between the TO and TA band that can be observed in Fig. 2. The interaction of the modes in our model for the bulk or the vacancy with H or F gives rise

to the wagging and stretching modes, ω_2^{xy} and ω_2^z, and two other modes at lower frequencies (see Table II). For both atoms, in which $\omega_2^z \gg \omega_1^z$, we can approximate the frequencies of the vibrations in the Si—X bond direction by

$$(\omega_1^z)^2 \simeq \frac{1}{3(M_{Si}+M_X)}(K_r+8K_\theta+8\beta K'_\theta) , \qquad (6a)$$

$$(\omega_2^z)^2 \simeq \frac{1}{\mu}K'_r . \qquad (6b)$$

The second is the stretching frequency of the Si—X bond whereas the first is a perturbation of the vibration (5b) of the Si atom in a vacancy induced by the presence of atom X. In the latter case, we can neglect for the Si—H bond the effect of M_H, and the perturbation is reduced to a hardening of the Si vibrations due to K'_θ. These modes, as can be seen in Fig. 3, are pushed up towards the TA upper edge singularity. We believe that this process is the main one responsible for the "quasilocal" vibrational mode observed in the ir spectra of a-Si:H at ~ 210 cm^{-1}. It is clear from Fig. 3, that a single Si—H bond in our unrelaxed vacancy model is not strong enough to make these states appear as a sharp resonance. However, any small perturbation in the surroundings of the Si—H bond can now give rise to a sharp peak in the TA band edge. In Ref. 6 the effect of small internal surfaces is discussed.

From Eq. (6a), we deduce that an increasing of the force constants describing the interactions among the four Si atoms of Fig. 1, due to relaxation or to the different electronegativity of the H and Si atoms, can also give rise to a strong "quasilocal" mode. In Fig. 8 we show the LDOS in the same Si atom that in Fig. 3, but with $K_r=1.43$ dyn cm^{-1} and $K_\theta=0.07$ dyn cm^{-1} in the cluster. Comparing the z component in Fig. 8 with that in Fig. 3, we can easily observe the strong effect of the perturbation in the force constants, due to the fact that the frequencies ω_2^z were already quite near the upper-band-edge TA singularity.

In Table II we also observe a slight shift to lower frequencies of the Si vibrations in the x-y plane when an H atom is bonded to it. This shift can be easily seen in the TO band of Fig. 3, and has been observed in the ir spectra of highly hydrogenated samples.[4] We can explain this feature as a result of the interaction of the localized wagging mode with the TO band of the Si atom. In the case of a-Ge:H the wagging mode is further away from the TO band at ~ 300 cm^{-1} and we expect this shift to be negligible, as can be easily obtained from Eqs. (2a) and (2b). Finally, inelastic neutron scattering experiments on a-Si:H

TABLE II. Vibrational frequencies obtained for bulk and surface silicon and for Si—H and Si—F bonds embedded in Si with the simple model discussed in the text.

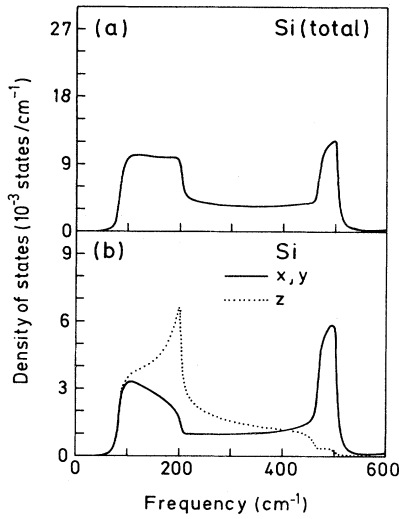| Mode		Bulk	Vacancy	Si—H	Si—F
	ω_1^z	344	182	202	163
	ω_2^z			2002	824
	ω_1^{xy}	344	334	323	137
	ω_2^{xy}			628	375

FIG. 8. Densities of states for the motion of Si in a Si—H bond embedded in a-Si:H as obtained with the Bethe-lattice method but with the force constants of Fig. 3 slightly modified as discussed in the text. The aim of this figure is to display the sharp peak in the z component of the DOS at the top of the TA band.

(Ref. 15) reveal an increase in the relative weight of the TO band with respect to pure a-Si. This can be easily understood by referring to Fig. 3(b), since the neutron scattering spectra in a-Si:H are more sensitive to the local density of vibrational states at the H atoms (the scattering cross section for H is ~ 50 times larger than that of Si).

In the case of the Si—F bond we can see in Table II that the in-phase vibration states in the direction of the bond are not shifted to higher frequencies with respect to the vacancy. The effect of K'_θ in Eq. (6a) is, in this case, compensated by the large mass of the F atoms. On the other hand, as we have shown before, the interaction of the wagging mode with the continuum spectrum gives rise to a peak at ~ 200 cm^{-1} and a shift in the TO band.

The different nature of the vibrational "resonance" of the upper edge of the TA band appears clearly when comparing Figs. 3 and 5: In the case of Si—H bonds, this resonance is polarized along z (longitudinal) while for Si—H bonds the polarization is transverse (x,y). The reason why these modes appear at the same frequency is that they occur near the TA singularity. The singularity traps defect modes which occur in its neighborhood. A better comparison with the ir experiments can be made if we calculate the absorption coefficient

$$\alpha(\omega) = \frac{2\pi}{n}\omega\epsilon_2(\omega) \tag{7}$$

where n is the index of refraction and ϵ_2 the imaginary part of the dielectric function. In the simplest possible model we can consider that the main contribution to ϵ_2 in a-Si:F comes from the ionicity of the Si—F bond. In this case we can write[16]

$$\epsilon_2(\omega) = -N_d 4\pi \left[\sum_{i,j} \text{Im}(\vec{\vec{Q}}_i \cdot \vec{\vec{G}}_{ij} \cdot \vec{\vec{Q}}_j) \right], \quad i,j = \text{Si,F} \tag{8}$$

where N_d is the density of Si—F bonds, $\vec{\vec{Q}}_i$ is the effective charge tensor in the Si or F atoms, and $\vec{\vec{G}}_{ij}$ the Green-function matrices described in the Appendix. The tensor $\vec{\vec{Q}}_i$, given by the derivatives of the dipole moment with respect to the atom displacements:

$$[Q_i]_{\alpha,\beta} = \frac{\partial M_\alpha}{\partial u_\beta(i)} \tag{9}$$

is assumed to be a diagonal tensor, with a longitudinal and two degenerate transverse elements, in the frame of reference of Fig. 1 (the bond along the z axis), whose elements can be obtained from molecular data.[17] Of the two sets of elements of the tensor $\vec{\vec{Q}}_i$ given in Ref. 17, we use $[Q_i]_{\text{long}} = 1.17e$ and $[Q]_{\text{trans}} = 0.68e$ as these values yield the best agreement with experimental data. Also, the other set implies that $[Q_i]_{\text{long}}$ and $[Q_i]_{\text{trans}}$ have opposite signs, a rather unpalatable situation. In Fig. 9 we show the calculated absorption coefficient and the experimental results for an F concentration of 10% (the one used in Fig. 5 of Ref. 11). The calculated results were slightly broadened by convoluting them with the Gaussian

$$G(\omega') = (2\sigma^2\pi)^{-1/2}\exp(-\omega'^2/2\sigma^2) \ .$$

The spurious low-frequency band-edge states (see Figs. 5 and 6) correspond to in-phase vibrations (see Fig. 7) and do not contribute to the absorption coefficient, the two main contributions coming from the wagginglike states at ~ 200 and 505 cm^{-1}. We have not included the background contribution of the Si bulk and other possible dipole contributions, such as the charge transfer of the back Si atoms that will increase the relative weight of the 505-cm^{-1} feature. The agreement with the experimental results is good except for the structure at ~ 300 cm^{-1}. One must keep in mind that the magnitudes of the absorption coefficient were obtained from the theory without fitting the experiment. The feature at 300 cm^{-1} can come either from the similar peak already existing in pure a-Si, whose ir activity is increased by the out-of-phase character of all the vibrations in this region (see Fig. 7), or from some modes of vibration associated with the Si-F$_2$ units.[18] None of these possible mechanisms are included in our model.
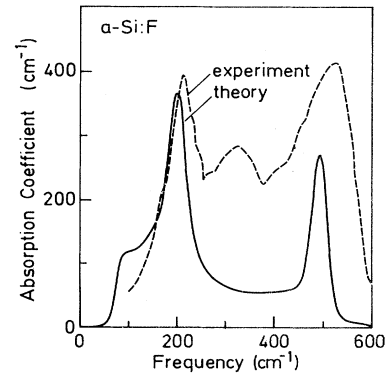

FIG. 9. Absorption spectrum of a-Si:F (with 10% fluorine) calculated with the Bethe-lattice method including only the vibration of the Si—F bonds. The results are compared with experimental data of Ref. 11.

The discrepancy between the calculated and the experimental curve in the region of the TO modes is due, in part, to having neglected in our calculation the dipole moment associated with the vibrations of the Si matrix.

Unfortunately, a similar estimate of the absorption spectrum of a Si:H around the TA band is not possible. The reason is that for this band the hydrogen moves almost exactly together with the silicon to which it is attached. As shown in Ref. 6, the dipole mechanism must involve changes in the back bonds. In view of the uncertainties and increasing number of free parameters involved in such mechanisms, we have not performed a detailed calculation of the absorption spectrum for the a-Si:H case. In the experimental spectra a strong peak appears at ~ 212 cm^{-1}.[11,12] Figure 8 shows that the peak is very weak for the total density of states although it appears strongly in its z component. We thus believe that the z-component ir coupling constant (e.g., the dipole matrix element) must be much larger than its x,y counterparts in order to fit the observed ir spectra.

The 212-cm^{-1} peak appears weakly in the Raman spectra, in a way which seems to reflect the total density of states of Fig. 8. Recent inelastic neutron measurements by Kamitakahara[15] have succeeded in observing the ~ 212 peak in a-Si:H. We partially reproduce his data in Fig. 10 in comparison with the projection of the DOS on the H atom (the main contribution to the scattering comes from the hydrogen). We believe that, in view of the shortcomings of the Bethe-lattice model, the calculated density of states accounts qualitatively for the neutron data. The weak part at the upper edge of the TA band seen in the experiment is seen in the z component of the calculated density of states but is rounded off in the "total" DOS. We do not know the exact experimental configuration but it is possible that the measured DOS is somewhat more sensitive to the longitudinal (z) DOS as a result of a preferential sample orientation.

The ability of our model to reproduce the ir spectrum of a-Si:F allows us to make some predictions for the ir spectrum of a-Ge:F. The force constants for the Ge—F bond can be extrapolated from those of the Si—F bond under the assumption that they scale from Si to Ge in the same way as those of the corresponding hydrogenated samples. In Table I we have included the force constants providing the best fit for a-Ge:H and the extrapolated ones for a-

FIG. 11. Infrared absorption and local DOS calculated for a-Ge:F with the parameters of Table I.

Ge:F. The results of our Bethe-lattice calculations for a-Ge:H and a-Ge:F are shown in Fig. 11. In this figure, we show the LDOS in the Ge and F atoms and the absorption coefficients for the a-Ge:F case. The stretching mode, not displayed in the figure, is expected to be at 680 cm^{-1}. We can appreciate two main differences with respect to the a-Si:F spectrum: (i) The wagginglike resonance spreads over to the longitudinal band, and (ii) the contribution of the F vibrations to the TO band is rather small, due to the larger mass of the Ge atoms.

V. CONCLUSIONS

We have shown that a simple cluster-Bethe-lattice calculation with second-order force constants can explain the quasilocal modes observed near the top of the TA band of a-Si:H and a-Si:F. The observed peaks, however, are shown to have different origins in the H and the F case. For a-Si:H the peak is mainly a rigid vibration of the Si—H bond longitudinal to the bond while for a-Si:F the vibration is transverse, related to the wagging mode of the Si—F bonds. In the latter case, we have calculated the absorption spectrum and obtained quantitative agreement with the strength of the observed absorption near the quasilocal mode. Thus, surface clusters of H, of the type proposed in Ref. 6, do not seem to be necessary to explain the quasilocal modes. They may, however, enhance the effect calculated here.

ACKNOWLEDGMENTS

APPENDIX

In our system (cluster and Bethe lattice) we have four different bond directions corresponding to the tetrahedral
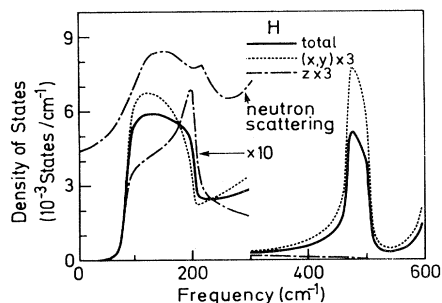

FIG. 10. Density of vibration states of a-Si:H at the H atoms compared with inelastic neutron scattering data of Kamitakahara (Ref. 15). The arrow shows the resonant mode discussed in the text.
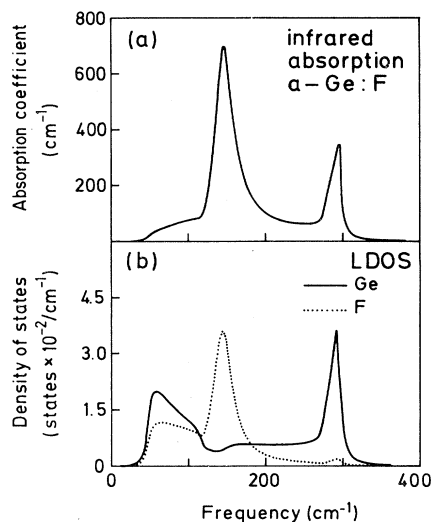
directions of Fig. 1. We label all the bonds from 1 to 4 depending on their direction, bonds 1 being those in the Si—X bond direction. All the atoms of the system can be labeled as $(i,j,k \cdots x,y)$ the notation indicating the path of bonds we have to follow to reach a given atom from the Si atom (labeled as 0) attached to atom X. Let $\underline{G}_{h,ijk\cdots x}$ be the 3×3 set of matrix elements of the Green functions between the vibrations of atom h of the cluster and atom $ijk \cdots x$. In the Bethe lattice these matrix elements are related by [see Eq. (18) or Ref. 9]

$$\underline{G}\cdots_{ijk}=T_k^i\underline{G}\cdots_{jk}+\underline{T}_{k,j}\underline{G}\cdots_j \ . \tag{A1}$$

In Eq. (A1) $\underline{T}_k^j$ and $\underline{T}_{kj}$ $(j\neq k)$ are the transfer matrices that can be obtained by iteration using the following equations:

$$\underline{T}_k^j=\underline{\Delta}_k\left[\underline{D}_k+\sum_{l\,(\neq k)}\left[\underline{D}_l+\sum_{m\,(\neq l)}\underline{B}_{km}\underline{T}_m^l\right]\underline{T}_{lk}\right.$$
$$\left.+\sum_{l\,(\neq k,j)}\underline{B}_{kl}\underline{T}_e^j\right], \tag{A2a}$$

$$\underline{T}_{kj}=\underline{\Delta}_k\left[\underline{B}_{kj}+\sum_{l\,(\neq k,j)}\underline{B}_{kl}\underline{T}_{lj}\right], \tag{A2b}$$

where

$$\underline{\Delta}_k=\left\{\underline{D}_0-\sum_{l\,(\neq k)}\left[\left[\underline{D}_l+\sum_{m\,(\neq l)}\underline{B}_{lm}\underline{T}_m^l\right]\underline{T}^k\right.\right.$$
$$\left.\left.+\sum_{m\,(\neq l)}\underline{B}_{lm}\underline{T}_{ml}\right]\right\}^{-1}. \tag{A3}$$

$\underline{D}_i$ and $\underline{B}_{ij}$ are the first- and second-neighbor interaction matrices, respectively, through bonds i and j. These matrices can be easily obtained as the second derivatives of the potential energy in (1) with respect to the atomic displacements. $\underline{D}_0$ is the "self-energy" matrix defined as

$$\underline{D}_0=M\omega^2\underline{1}-\sum_{i=1}^4\left[\underline{D}_i+\sum_{j\,(\neq i)}\underline{B}_{ij}\right], \tag{A4}$$

with M the mass of the Si (Ge) atom.

The vibration of the five-atom cluster and its connection with the bulk can be described by the 15×15 matrix $\underline{M}$

$$\underline{M}=\begin{bmatrix}\underline{\delta}_0 & \underline{D}_1' & \underline{\delta}_2 & \underline{\delta}_3 & \underline{\delta}_4 \\ (\underline{D}_1')^T & \underline{D}_{0,1} & \underline{B}_{12}' & \underline{B}_{13}' & \underline{B}_{14}' \\ (\underline{\delta}_2)^T & \underline{B}_{21}' & \underline{\delta}_0^2 & \underline{B}_{23} & \underline{B}_{24} \\ (\underline{\delta}_3)^T & \underline{B}_{31}' & \underline{B}_{32} & \underline{\delta}_0^3 & \underline{B}_{34} \\ (\underline{\delta}_4)^T & \underline{B}_{41}' & \underline{B}_{42} & \underline{B}_{43} & \underline{\delta}_0^4\end{bmatrix} \tag{A5}$$

where

$$\underline{\delta}_0=\underline{D}_{0,0}-\sum_{i=2}^4\sum_{j(\neq i)}\underline{B}_{ij}\underline{T}_{ji} \ , \tag{A6a}$$

$$\underline{\delta}_0^i=\underline{D}_{0,i}-\sum_{j(\neq i)}\left[\left[\underline{D}_j+\sum_{k(\neq j)}\underline{B}_{jk}\underline{T}_k^j\right]\underline{T}_j^i\right.$$
$$\left.+\sum_{k(\neq j)}\underline{B}_{jk}\underline{T}_{kj}\right], \tag{A6b}$$

$$\underline{\delta}_i=\underline{D}_i'+\sum_{j(\neq i)}\underline{B}_{ij}\underline{T}_j^i \ . \tag{A6c}$$

$\underline{D}_i'$ and $\underline{B}_{1j}'$ are the interaction matrices through K_r' and K_θ' in the cluster. They are given by[19]

$$\underline{D}_1'=-\begin{bmatrix}\alpha_1 & \beta_1 & \beta_1 \\ \beta_1 & \alpha_1 & \beta_1 \\ \beta_1 & \beta_1 & \alpha_1\end{bmatrix} \ ,$$

$$\underline{D}_2'=-\begin{bmatrix}\alpha_2 & -\beta_2 & -\beta_2 \\ -\beta_3 & \alpha_3 & \beta_4 \\ -\beta_3 & \beta_4 & \alpha_3\end{bmatrix} \ ,$$

$$\underline{B}_{12}'=-\frac{K_\theta'}{6}\begin{bmatrix}-4 & -2 & -2 \\ 2 & 1 & 1 \\ 2 & 1 & 1\end{bmatrix} \ ,$$

$$\alpha_1=\tfrac{1}{3}[K_r'+(1+3/\beta)K_\theta'] \ ,$$

$$\alpha_2=\tfrac{1}{3}[K_r+4K_\theta+2(1+\beta)K_\theta'] \ ,$$

$$\alpha_3=\tfrac{1}{3}[K_r+8K_\theta-\tfrac{1}{2}(1-\beta)K_\theta'] \ ,$$

$$\beta_1=\tfrac{1}{3}[K_r'-\tfrac{1}{2}(1+3/\beta)K_\theta'] \ ,$$

$$\beta_2=\tfrac{1}{3}[K_r-2K_\theta-(1+\beta)K_\theta'] \ ,$$

$$\beta_3=\tfrac{1}{3}[K_r-4K_\theta+(1-\beta)K_\theta'] \ ,$$

$$\beta_1=\tfrac{1}{3}[K_r-4K_\theta-\tfrac{1}{2}(1-\beta)K_\theta'] \ .$$

$\underline{D}_{0,h}$ $(h=0,\ldots,4)$ are the "self-energy" matrices of the five atoms in the cluster. The inverse of matrix $\underline{M}$, equivalent to Eq. (33) of Ref. 9, contains all the information on the vibration of the cluster. Its diagonal elements (actually 3×3 matrices corresponding to the three cartesian coordinates) are proportional to the density of vibrational states at each of the cluster atoms projected along the appropriate cartesian directions and the off-diagonal elements are proportional to the correlation functions.

---

*Permanent address: Departamento de Física Fundamental, Universidad Autónoma de Madrid, Cantoblanco E, Madrid 34, Spain.
[1]G. A. N. Connell and J. R. Pawlik, Phys. Rev. B 13, 787 (1976); C. C. Tsai, H. Fritzsche, M. H. Tanielian, P. J. Gaczi, D. D. Persans, and M. A. Vesaghi, in *Amorphous and Liquid Semi-conductors*, edited by W. E. Spear (University of Edinburgh, Edinburgh, 1978), p. 339; G. Lucovsky, R. J. Nemanich, and J. C. Knights, Phys. Rev. B 19, 2064 (1979); J. C. Knights and G. Lucovsky, in Crit. Rev. Solid State Mater. Sci. 9, 210 (1980).
[2]M. H. Brodsky, M. Cardona, and J. J. Cuomo, Phys. Rev. B 16,

3556 (1977).

[3]S. C. Shen, C. J. Fang, and M. Cardona, Phys. Status Solidi B <u>101</u>, 451 (1980).

[4]S. C. Shen, C. J. Fang, M. Cardona, and L. Genzel, Phys. Rev. B <u>22</u>, 2913 (1980).

[5]D. Bermejo and M. Cardona, J. Non-Cryst. Solids <u>32</u>, 405 (1979).

[6]E. Martínez and F. Ynduráin, Solid State Commun. <u>44</u>, 1477 (1982).

[7]F. Ynduráin, J. D. Joannopoulos, M. L. Cohen, and L. Falicov, Solid State Commun. <u>15</u>, 617 (1974).

[8]J. D. Joannopoulos and F. Ynduráin, Phys. Rev. B <u>10</u>, 5164 (1974).

[9]D. C. Allan, J. D. Joannopoulos, and W. B. Pollard, Phys. Rev. B <u>25</u>, 1065 (1982). Other studies of the vibrational spectra of a-Si using the cluster-Bethe-lattice method can be seen in B. K. Agrawal, Phys. Rev. Lett. <u>46</u>, 774 (1981); W. B. Pollard and J. Joannopoulos, Phys. Rev. B <u>23</u>, 5263 (1981); W. B. Pollard and G. Lucovsky, in *Amorphous and Liquid Semicon-*

ductors, edited by B. K. Chakraverty and D. Kaplan (Les éditions de Physique, Les Ulis, France, (1981), p. 353.

[10]W. Weber, Phys. Rev. B <u>15</u>, 4789 (1977).

[11]H. Shanks, C. J. Fang, L. Ley, M. Cardona, F. J. Demond, and S. Kalbitzer, Phys. Status Solidi B <u>100</u>, 43 (1980).

[12]C. J. Fang, L. Ley, H. R. Shanks, K. J. Gruntz, and M. Cardona, Phys. Rev. B <u>22</u>, 6140 (1980).

[13]T. Shimada, Y. Katayama, and S. Horigome, Jpn. J. Appl. Phys. <u>19</u>, L265 (1980).

[14]M. Cardona, Phys. Status Solidi (in press).

[15]W. A. Kamitakahara, private communication (unpublished).

[16]See, for instance, M. Cardona, in *Light Scattering in Solids II* (Springer, Heidelberg, 1982), p. 58.

[17]P. N. Schatz and D. F. Hornig, J. Chem. Phys. <u>21</u>, 1516 (1953).

[18]G. Lucovsky, *Fundamental Physics of Amorphous Semiconductors,* edited by F. Yonezawa (Springer, Berlin, 1981).

[19]M. J. P. Musgrave and J. A. Pople, Proc. R. Soc. London Ser A <u>268</u>, 474 (1962).